

Experimental Study on Surge Propagation Characteristics of Rail and Lightning Overvoltages on Level Crossing

Hideki Arai* Member
 Hiroji Matsubara* Member
 Kiyotomi Miyajima* Member
 Shigeru Yokoyama* Member
 Kazutoshi Sato** Member

Lightning protection measures are required for the railway signalling system because suspension and delays of trains due to lightnings may cause social confusion. Therefore, we carried out experiments on propagation characteristics of lightning surges along a rail, and injected a lightning surge current into the rail or wayside ground to raise their potentials, in order to measure the lightning overvoltages on a level crossing for the insulation design. There are no precedents that have carried out these experiments in the field until now. We could obtain the following results.

- (1) The surge impedance of the rail is 56Ω and the surge propagation velocity in the rail is $55\text{ m}/\mu\text{s}$.
- (2) The surge attenuation depends only on the duration of wave tail of the traveling lightning surge along the rail and decreases as the duration of wave tail becomes longer.
- (3) Flashovers may occur at the terminals in the equipment of the level crossing in case 1) a 2 kA lightning surge current is directly injected into the rail, or 2) a 10 kA lightning surge current is injected into the wayside ground at a vertical distance of 2 m from the rail.
- (4) We can estimate the lightning overvoltages on the terminals in the equipment of the level crossing according to the vertical distance from the rail of the lightning stroke and the level of the stroke current.

Keywords: lightning surge, propagation characteristics, rail, lightning overvoltages, railway signalling system, level crossing

1. Introduction

The railway signalling system has made remarkable progress in recent years in electric railways with their components becoming increasingly compact and multi-functional due to the adoption of microcomputers and other electronic devices in wide ranges. On the other hand, burning of circuits, system-down, and other lightning damages on the railway signalling system frequently occur because electronic devices are easily broken by lightning surges.

The railway signalling system is widely installed at a wayside and constitutes a network by being connected each other with rails and cables. Accordingly, there are a lot of parts that lightning surges can invade easily. In addition, troubles extend to wide ranges in case of occurring lightning damages on the railway signalling system.

Therefore, it is required to build up effective and economical countermeasures for preventing lightning damages on the railway signalling system since suspension

and delays of trains due to lightnings may cause social confusion.

Since the railway signalling system is usually installed at a wayside and directly connected to rails through cables, the rail can be one of the invasion routes of lightning surges to the railway signalling system. Therefore, it is important to clarify propagation characteristics of lightning surges along the rail in order to establish lightning protection measures for the railway signalling system.

Accordingly, we carried out experiments on the following.

- (1) Measurement of the surge impedance of the rail and the surge propagation velocity in the rail
- (2) Measurement of the surge attenuation ratio in the rail
- (3) Measurement of the wayside ground potential distribution caused by the rail potential rise

Moreover, we temporarily installed an actual level crossing, and injected a lightning surge current into the rail or wayside ground to raise their potentials, in order to measure the lightning overvoltages on the level crossing so that we can obtain basic data for the insulation design.

There are no precedents that have carried out these

* Komae Labs., Central Research Institute of Electric Power Industry
 2-11-1, Iwado Kita, Komae-shi, Tokyo 201-8511

** Railway Technical Research Institute
 2-8-38, Hikari-cho, Kokubunji-shi, Tokyo 185-8540

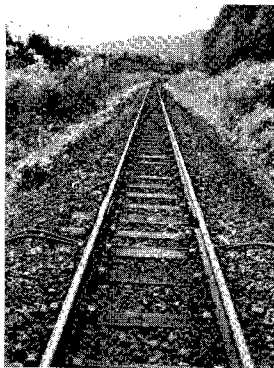


Fig. 1. Test section

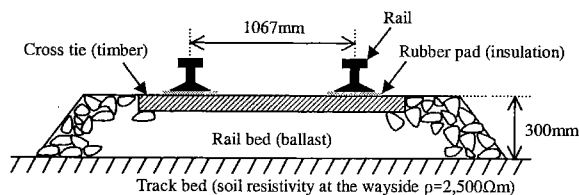


Fig. 2. Line profile of the test section

experiments in the field until now.

This paper describes the results of the above field tests.

2. Outline of Field Tests

2.1 Test Section We carried out field tests between Ginzan and Shikaribetsu stations, Hakodate line of JR Hokkaido. Fig.1 shows the test section. We selected a non-electrified and single track section as the test section because noises induced on rails could be reduced in the measurement.

2.2 Railway Track Conditions Fig.2 shows the line profile of the test section. A railway track consists of rails, cross ties, a rail bed, and a track bed. This test section consists of timber cross ties and a ballast rail bed. The rail is basically insulated from cross ties by rubber pads. The soil resistivity was 2,500Ωm at the wayside. The field tests were done on a fine day when both the rail and rail bed were dry.

3. Surge Impedance of the Rail and Surge Propagation Velocity in the Rail

3.1 Measuring Method Fig.3 shows an outline of measuring method. The length of rail for measuring is 329m. Two measuring rails are insulated from adjacent rails by inserting insulated rail joints at both ends as shown in Fig.3. A steep-front current generated by a pulse generator (PG) was injected into the sending end of one side rail (for example the rail No.1 in Fig.3). Then, the injected current waveform (I), voltage waveform of the rail No.1 (V_s), and voltage waveform of the rail No.2 (V_m) were measured with an oscilloscope. The self surge impedance of the rail No.1, mutual surge impedance between rails No.1 and No.2, and surge propagation velocity in the rail No.1 were calculated from measured waveforms.

The same measurement as the above-mentioned was

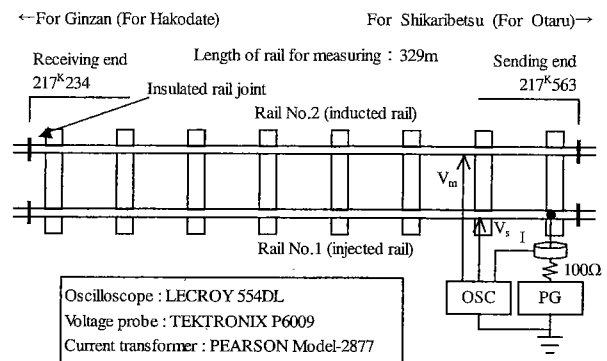


Fig. 3. Outline of measuring surge parameters of the rail

implemented with a steep-front current injected into the rail No.2.

3.2 Measured Results The self and mutual surge impedances of rails No.1 and No.2 are as follows.

$$Z = \begin{pmatrix} 56.8 & 43.2 \\ 42.6 & 55.8 \end{pmatrix} \cong \begin{pmatrix} 57 & 43 \\ 43 & 56 \end{pmatrix} (\Omega)$$

When the geometrical arrangement of two rails are considered, the surge impedance matrix should become a symmetric matrix. There is a little difference, however, because of measurement errors.

Moreover, both the round trip surge propagation times on rails No.1 and No.2 were 12μs. Accordingly, the surge propagation velocity in the rail is 55 m/μs.

As a result, it is clarified that the self surge impedance of the rail with timber cross ties and a ballast rail bed is extremely low compared with that of an overhead line⁽¹⁾. In addition, the surge propagation velocity in the rail is 18.3% of the light velocity and is similar to that in a buried conductor⁽²⁾.

4. Surge Attenuation Ratio in the Rail

A lightning surge voltage of an arbitrary waveform generated by a PG was impressed to the sending end of the rail No.1 as shown in Fig.3. Then, the voltage waveform of the rail No.1 (V_{ss}) was measured with an oscilloscope at the sending end. In the same way, the voltage waveform of the rail No.1 (V_{rs}) was measured at the receiving end. Supposing that the impressed lightning surge voltage reflects perfectly on the insulated rail joint at the receiving end, we defined the surge attenuation ratio in the rail as Eq. (1).

$$\begin{aligned} & \text{(Surge attenuation ratio)} \\ & = (\text{Wave crest of } V_{rs}) / (2 \times \text{Wave crest of } V_{ss}) \end{aligned} \quad \dots \dots \dots (1)$$

Namely, Eq. (1) indicates that this surge attenuation ratio becomes lower as the attenuation of the lightning surge voltage caused by traveling along the rail increases.

The surge attenuation ratio in the rail was measured as parameters of the duration of wave front (T_f) and wave tail (T_t) of the lightning surge voltage impressed to the rail No.1.

Fig.4 shows the measured voltage waveforms of V_{ss}

and V_{rs} when a $1/40 \mu\text{s}$ lightning surge voltage was impressed to the rail No.1. Fig. 4 indicates that the wave crest decreases and T_f becomes longer as a lightning surge voltage travels along the rail.

Fig. 5 shows the measured results of T_t -dependence of the surge attenuation ratio. On the other hand, Fig. 6 shows the measured results of T_f -dependence of that ratio. From Figs. 5 and 6, the surge attenuation ratio depends only on T_t and increases as T_t becomes longer, because the wave crest is decided at the wave tail in the case of distorting the wave front of the voltage waveform at the receiving end as shown in Fig. 7.

Although the soil resistivity of this test section was as high as $2,500 \Omega\text{m}$, it can be thought that the attenuation of the lightning surge voltage caused by traveling along the rail decreases if the rail is laid on the site with low soil resistivity.

As a result, it is clarified that the attenuation of a

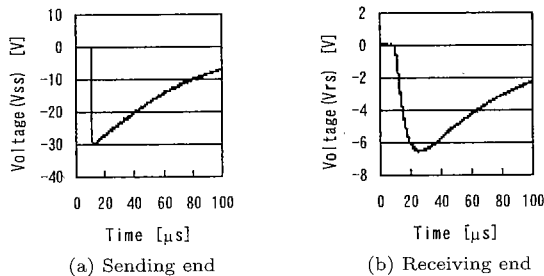


Fig. 4. Measured voltage waveforms at the sending and receiving ends of the rail No.1 at an impressed lightning surge voltage of $1/40 \mu\text{s}$

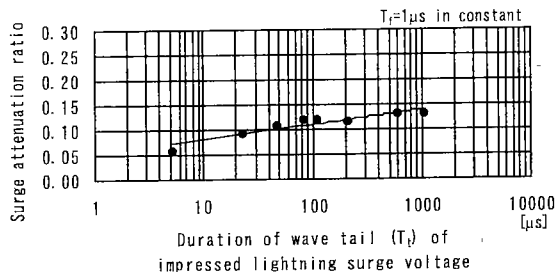


Fig. 5. T_t -dependence of the surge attenuation ratio

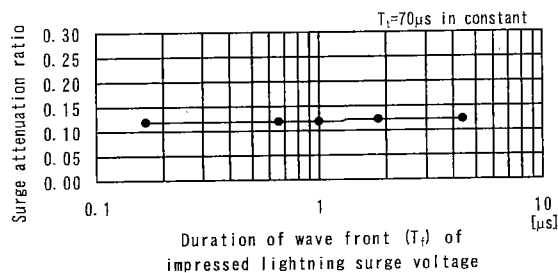


Fig. 6. T_f -dependence of the surge attenuation ratio

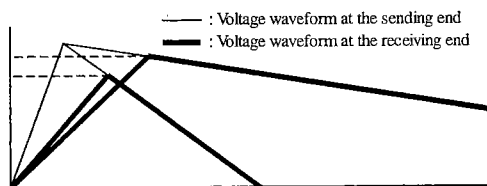


Fig. 7. Reason for T_t -dependence of the surge attenuation ratio

lightning surge voltage caused by traveling along the rail is extremely large compared with that of an overhead line. Rails may have extremely high leakage conductance against the ground in comparison with overhead lines.

5. Wayside Ground Potential Distribution caused by a Rail Potential rise

5.1 Measuring Method Fig. 8 shows an outline of measuring method. A rail potential rise was caused when a $1/70 \mu\text{s}$ lightning surge current generated by an impulse generator (IG) was injected into Point A of the rail No.1. Then, the potential rises of the rail No.1, rail No.2, and wayside ground against a remote potential electrode were measured with an oscilloscope at Points A, B, and C, respectively. The measuring points are illustrated by ● in Fig. 8. They are indicated by the horizontal distance for the rail from the current injecting point ($x=0 \text{ m}$ is Point A) and vertical distance from the rail No.1 ($y=0 \text{ m}$ is the rail No.1).

5.2 Measured Results Fig. 9 shows the relationship between the potential rise of the rail or wayside ground and the horizontal distance from the current injecting point. The Y-axis of Fig. 9 indicates the potential rises at an injected lightning surge current of 1 A (wave crest).

Fig. 9 shows that there are few differences in the potential rise of the rail or wayside ground between $x=0 \text{ m}$ and $x=10 \text{ m}$. However, the potential rises of the rail and wayside ground at Points B and C are lower than those at Point A. Thus, an injected lightning surge current travels along the rail without attenuation for approximately $x=10 \text{ m}$, but attenuates as mentioned in the chapter 4 when it travels further.

Moreover, the potential rises of the rail No.2 and

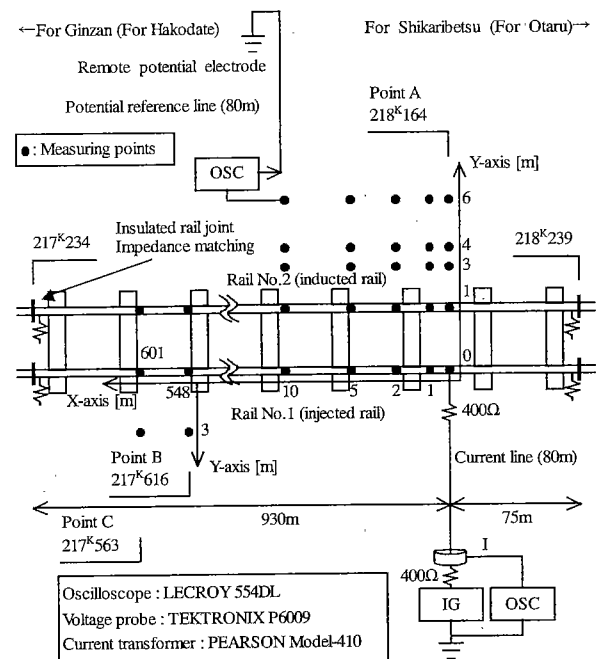


Fig. 8. Outline of measuring the wayside ground potential distribution

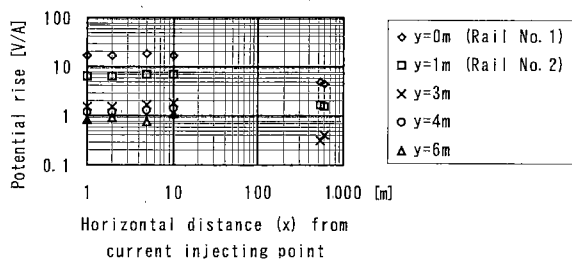


Fig. 9. Relationship between the potential rise of the rail or wayside ground and the horizontal distance from the current injecting point

wayside ground are induced in parallel with the potential rise of the rail No.1. The potential difference between the rail No.1 and the wayside ground at a vertical distance of 3 m from the rail No.1 is approximately 80% of the rail No.1 potential rise. This potential difference may be charged in the ballast rail bed because it exists for a vertical distance of about 3 m from the rail with very low conductivity compared with that of the ground.

Although the potential rises at $y=0$ m and $y=1$ m when $x=1$ m in Fig. 9 should theoretically be a half of the self and mutual surge impedances of rails, respectively, they became lower. It can be thought as the reason for this result is that rubber pads between rails and cross ties shown in Fig. 2 became contact electrically because the voltage impressed to the rail raised in the measurement of the wayside ground potential distribution higher than the measurement of the surge impedances.

As a result, it is clarified that the ground potential distribution near the rail is much different from that near a buried conductor⁽³⁾.

6. Lightning Overvoltages on Level Crossings

6.1 Measuring method Fig. 10 shows an outline of measuring method. An actual level crossing for lightning surge tests was installed temporarily. A potential rise of the rail or wayside ground was caused by injecting a $1/70 \mu\text{s}$ lightning surge current generated by an IG into Point A of the rail No.1 or wayside ground at a vertical distance of 2 m or 5 m from the rail No.1 as shown in Fig. 10. Then, the lightning overvoltages on each part of the level crossing against a remote potential electrode was measured with an oscilloscope at Points A, B, and C.

For a lightning stroke, it is supposed that the frequency of the wayside ground potential rise caused by striking structures such as steel beams for supporting feeders is higher than that of the rail potential rise caused by directly striking rails. In order to simulate a proximity lightning stroke as mentioned above, the case of the wayside ground potential rise was tested.

Fig. 11 shows photographs of an electronic train detector (HC type) (for short HC-TD) installed at Point A and an electronic level crossing control unit (for short LC-CU) installed at Point C. The HC-TD is a sensor directly connected to the rail for detecting trains to close crossing gates, and the LC-CU is the main equipment in

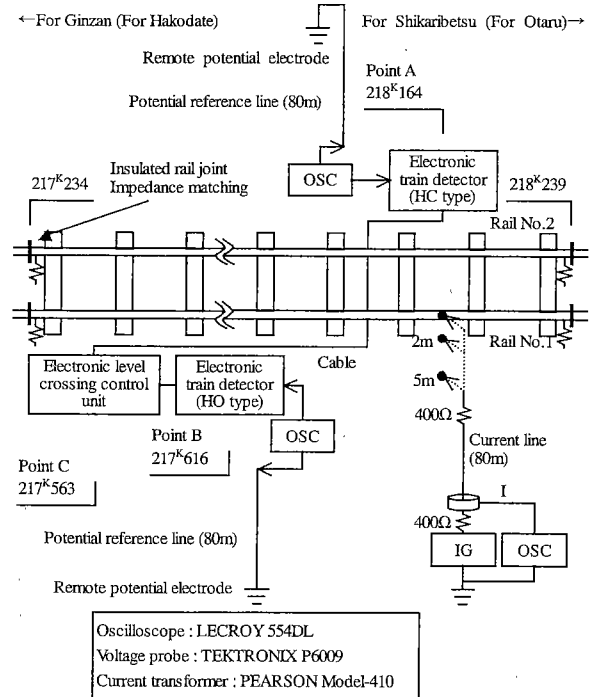
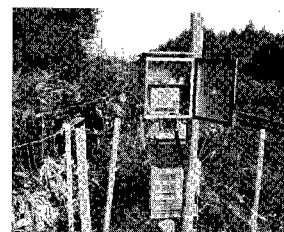


Fig. 10. Outline of measuring lightning overvoltages on the level crossing



(a) Electronic train detector (HC type)



(b) Electronic level crossing control unit

Fig. 11. Equipment of the level crossing

the level crossing for controlling crossing gates, warning lights, and speakers by the information of train detection from the HC-TD. Fig. 12 in the next page shows an outline of connection on the equipment of the level crossing. Lightning protection devices are also illustrated in Fig. 12.

6.2 Measured Results

(1) Measured lightning overvoltage waveforms on each part of the level crossing.

Fig. 13 shows the measured lightning overvoltage waveforms on the HC-TD and LC-CU at a rail potential rise. The Y-axis of Fig. 13 indicates the lightning overvoltages at an injected lightning surge current of 1 A (wave crest). The legends in Fig. 13 indicate the names of measuring terminals (refer to Fig. 12 in the next page).

The lightning overvoltages on the HC-TD in Fig. 13(a) are much higher than those on the LC-CU in Fig. 13(b). Therefore, the potential difference between the HC-TD and LC-CU generates. In this test, the lightning surge currents injected into the rail are approximately 10 A to minimize the influence on the other operating system of railway. Accordingly, lightning protection devices illustrated in Fig. 12 could not perform. If

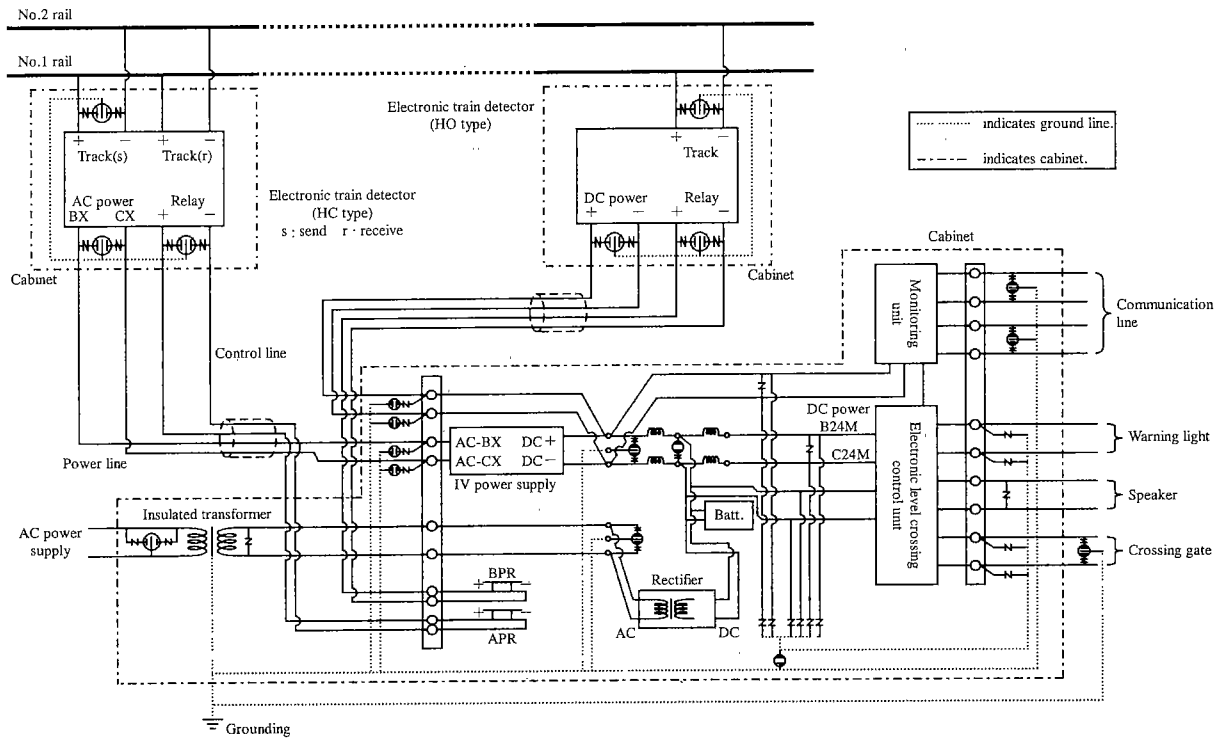
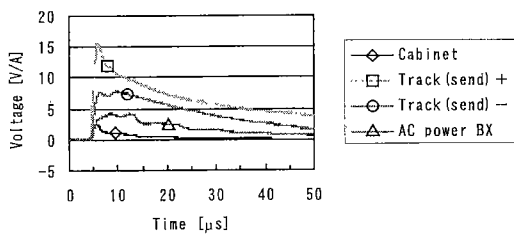
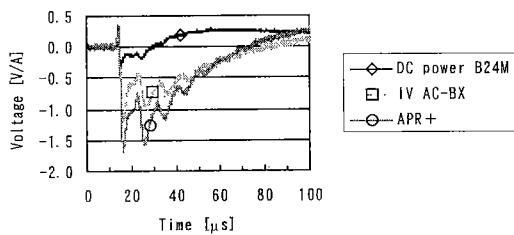


Fig. 12. Outline of connection on the equipment of the level crossing



(a) Electronic train detector (HC type)



(b) Electronic level crossing control unit

Fig. 13. Measured lightning overvoltage waveforms on the equipment of the level crossing at a rail potential rise

these lightning protection devices perform at a lightning stroke, a lightning surge current flows from the HC-TD to the LC-CU in order to reduce the potential difference in between.

(2) Lightning overvoltages on the level crossing at a proximity lightning stroke Fig. 14 shows the measured results of lightning overvoltages on each part of the level crossing at a potential rise of the rail or wayside ground. The Y-axis of Fig. 14 indicates the lightning overvoltages at a lightning surge current of 1 A (wave crest) directly injected into the rail for the rail potential rise, or at a lightning surge current of 1 A (wave crest) into the grounding of 100 Ω near the rail for the wayside ground

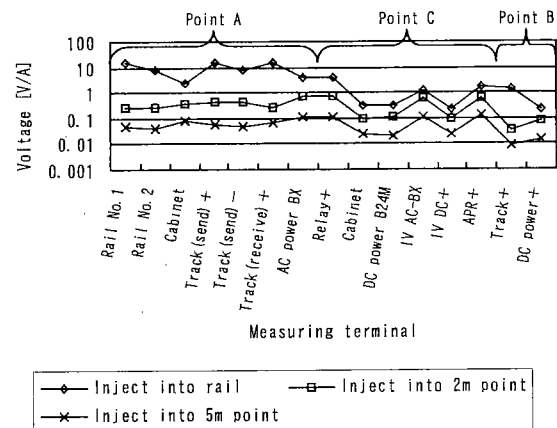


Fig. 14. Measured results of lightning overvoltages on the level crossing

potential rise.

Fig. 14 shows that the lightning overvoltages on each part of the level crossing becomes lower almost proportionally as the current injecting point is set more distant from the rail in the vertical direction.

Next, Fig. 15 shows the relationship between the lightning overvoltages on the power source terminals in the HC-TD installed at Point A or LC-CU installed at Point C and the vertical distance from the rail of the current injecting point.

Supposing that the flashover voltage of the AC power BX terminal in the HC-TD is 10 kV, Fig. 15 indicates that a flashover may occur at this terminal in case 1) a 2 kA lightning surge current is directly injected into the rail, or 2) a 10 kA lightning surge current is injected into the wayside ground at a vertical distance of 2 m from the rail No.1. Therefore, it needs lightning

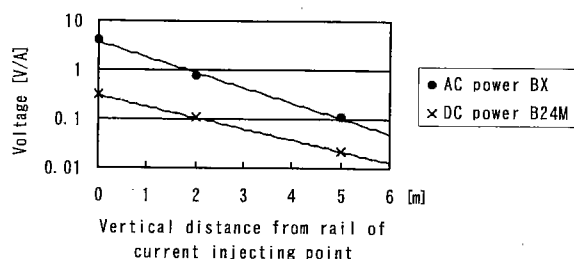


Fig.15. Relationship between the vertical distance from the rail of the current injecting point and the lightning overvoltages on the power source terminals of the level crossing

protection measures for this terminal. In this way, we can use Fig. 15 to estimate the lightning overvoltages on the power source terminals in the equipment of the level crossing according to the vertical distance from the rail of the lightning stroke and the level of the stroke current.

7. Conclusions

We carried out experiments on propagation characteristics of lightning surges along a rail, and injected a lightning surge current into the rail or wayside ground to raise their potentials, in order to measure the lightning overvoltages on a level crossing. There are no precedents that have carried out these experiments until now.

The main conclusions are summarized as follows:

(1) The surge impedance of the rail is $56\ \Omega$ and the surge propagation velocity in the rail is $55\text{ m}/\mu\text{s}$.

(2) The surge attenuation depends only on the duration of wave tail of the traveling lightning surge along the rail and decreases as the duration of wave tail becomes longer.

(3) Flashovers may occur at the terminals in the equipment of the level crossing in case 1) a 2 kA lightning surge current is directly injected into the rail, or 2) a 10 kA lightning surge current is injected into the wayside ground at a vertical distance of 2 m from the rail.

(4) We can estimate the lightning overvoltages on the terminals in the equipment of the level crossing according to the vertical distance from the rail of the lightning stroke and the level of the stroke current.

We will investigate methods of calculating surge parameters of the rail that reflect these experimental results. Moreover, we will investigate surge analysis models for level crossings to develop lightning protection designs.

Acknowledgment

The authors would like to thank the staff of Electric System Div., Engineering Dept. and Sapporo Signalling & Telecommunications Center, Hokkaido Railway Company, for their cooperation in these field tests.

(Manuscript received Feb. 27, 2003,

revised June 9, 2003)

References

- (1) A. Ametani: "Distributed-Parameter Circuit Theory",

Corona Publishing Co., Ltd., Tokyo (1990) (in Japanese)

- (2) H. Motoyama and T. Noda: "Experimental study on lightning surge characteristics of a buried bare wire", CRIEPI Report, No.T00062 (2001) (in Japanese)
- (3) CRIEPI Subcommittee for Power Stations and Substations, Lightning Protection Design Committee: "Guide to lightning protection design of power stations, substations and underground transmission lines", CRIEPI Report, No.T40 (1996) (in Japanese)

Hideki Arai (Member) was born on January 12, 1970. He



received the B.S. and M.S. degrees in information science from Tohoku University, Japan in 1992 and 1994, respectively. He joined Railway Technical Research Institute, Tokyo, Japan in 1994. He has been on loan to Central Research Institute of Electric Power Industry, Tokyo, Japan since 2000. He has been engaged in the research of lightning protection for railway signalling system.

Hiroji Matsubara (Member) was born on January 14, 1951. He graduated from Hachinohe Industrial college in 1971. In the same year, he



joined Central Research Institute of Electric Power Industry, Tokyo, Japan. He has been engaged in the researches of lightning surge analysis and lightning protection for power stations, substations, and transmission system.

Kiyotomi Miyajima (Member) was born on September 19, 1972. He received the B.S. and M.S. degrees from Tokyo University of Agriculture and Technology, Tokyo, Japan in 1995 and 1997, respectively. He joined Central Research Institute of Electric Power Industry, Tokyo, Japan in 1997. He has been engaged in the research of EMC of power system.



Shigeru Yokoyama (Member) was born on March 5, 1947. He received the B.S. and Ph.D. degrees from the University of Tokyo, Japan in 1969 and 1986, respectively. He joined Central Research Institute of Electric Power Industry, Tokyo, Japan in 1969 and since then, he has been engaged in the researches of lightning protection and insulation coordination of distribution and transmission system. He holds the posts of Associate Vice President in Komae

labs., of CRIEPI and Professor at Kyushu University concurrently since 2001. He is a Fellow of IEEE.



Kazutoshi Sato (Member) was born on October 16, 1956. He received the B.S. degree from Niigata University, Japan in 1979. In the same year, he



joined Japan National Railway, Tokyo, Japan. He is currently Railway Technical Research Institute, Tokyo, Japan since 1985. He has been engaged in the research of railway signalling system.